

# Comparison of Mono- to Diphosphate Ester Ratio in Inhibitor Formulations for Mitigation of Under Deposit Corrosion

Bruce Brown,<sup>†\*</sup> Amr Saleh,<sup>\*</sup> and Jeremy Moloney<sup>\*\*</sup>

## ABSTRACT

Mitigation of localized under deposit corrosion (UDC) in upstream oil and gas pipelines is an important research topic for both industry and academia. In a research program to better define the various inhibitor components that provide mitigation of UDC, this initial research investigates the effect of varied ratios of mono- to dinonylphenol phosphate esters (PE) by testing a set of specifically formulated inhibitors. Inhibitors with three mono- to di-PE ratios were tested in the presence and absence of 2-mercaptoethanol (ME). Using two 1.25 in (3.18 cm) diameter API 5L X65 pipeline steel samples and 250  $\mu\text{m}$  silica sand, UDC testing was conducted for 28 d in a  $\text{CO}_2$  saturated solution at 70°C and 1 bar (100 kPa) total pressure. Analysis has shown that localized corrosion (pit penetration rate) increased for ME-free nonylphenol PE as the concentrations of di-PEs and mono-PEs approached equivalency. The nonylphenol PE inhibitor with a 50:50 mono- to di-PE ratio at 100 ppm concentration failed to protect the surface of the sample under the individual sand grains. Even the base product inhibitor package with no PE provided better mitigation under these test conditions than the 50:50 mono- to dinonylphenol PE. However, it was observed that the addition of ME provided a dramatic improvement in the mitigation of UDC for each mono- to di-PE ratio of the nonylphenol PE tested. From this research, it is seen that the mono- to di-PE ratio is important to consider when developing corrosion inhibitors containing PEs.

**KEY WORDS:** API 5L X65, corrosion mitigation, nonylphenol, phosphate ester, under deposit corrosion

## INTRODUCTION

Under deposit corrosion (UDC) is a localized corrosion that occurs where sediments, carried through a production or transmission pipeline, have settled in stagnant or low-flow sections of a pipeline and mitigation strategies are ineffective or impractical. Computational fluid dynamics studies<sup>1-2</sup> have recently been conducted to understand mechanisms of solids deposition in order to mitigate deposit formation. Conclusions from these studies confirmed specific conditions related to flow and pipeline geometry reduce the near-wall velocity at the pipe floor, allowing deposits containing a mixture of water, hydrocarbons, microorganisms, and inorganic compounds to form. Particular types of inorganic deposits, i.e., silica sand, have been found to retard uniform corrosion of mild steel by slowing down the mass transfer of corrosive species;<sup>3</sup> however, the difference between the environmental conditions in the bulk solution versus under the deposit has been found to increase the probability of localized corrosion. This difference in environmental conditions is particularly prominent when an inhibitor is present in the bulk solution, as the sand deposit will slow down inhibitor diffusion to the metal surface, as well as parasitically deplete the inhibitor concentration through adsorption on the large surface area provided by the sand.<sup>4-5</sup> Even though an inhibitor has been shown to be effective in protecting the pipeline

Submitted for publication: May 26, 2015. Revised and accepted: September 21, 2015. Preprint available online: September 21, 2015, <http://dx.doi.org/10.5006/1786>.

<sup>†</sup> Corresponding author. E-mail: [brownb1@ohio.edu](mailto:brownb1@ohio.edu).

<sup>\*</sup> Institute for Corrosion and Multiphase Technology, Department of Chemical & Biomolecular Engineering, Ohio University, 342 W. State St., Athens, OH 45701.

<sup>\*\*</sup> NALCO Champion, 7705 Highway 90-A, Sugarland, TX 77478.

from uniform corrosion under sand beds, it may have a tendency to cause localized corrosion; therefore, care must be taken to evaluate each inhibitor's effectiveness before use.<sup>5</sup> A well-known example reported by Smart<sup>6</sup> found significant localized pitting under the sediment in the bottom of an inhibited crude oil transmission pipeline, while general corrosion rates in the pipeline were measured in the range of 0.005 mm/y to 0.01 mm/y (0.2 mpy to 0.4 mpy).

Laboratory experiments focused on UDC in a sweet environment have found that the addition of an inhibitor will not always mitigate localized corrosion and may lead to its acceleration. Marsh, et al.,<sup>7</sup> conducted artificial pit experiments using three industrial inhibitors in sweet conditions under a barium sulfate scale and found that low concentrations of the inhibitors (10 ppm) would give efficient general corrosion inhibition, but could lead to an acceleration of corrosion processes associated with galvanic phenomena. Pedersen, et al.,<sup>8</sup> investigated the risk of localized UDC of an X65 pipeline steel by galvanically coupling a sand-covered sample with a non-covered sample in the presence of an imidazoline-type inhibitor. When sand deposition occurred prior to adding the inhibitor, severe localized corrosion was observed with pit penetration rates of 4 mm/y to 5 mm/y, while the general corrosion rate was 0.2 mm/y. However, when the sand deposition occurred after both samples were exposed to the inhibitor, the corrosion rate was not greatly affected. In experiments using multi-electrode array probes, Hinds, et al.,<sup>9</sup> found that the addition of an inhibitor polarized a non-sand-covered electrode to a more noble potential with respect to a sand-covered electrode that accelerated the corrosion rate under the sand deposit. Even though the full composition of the two different inhibitors used in the study was unknown, it was shown that a significant amount of each inhibitor was lost by adsorption on the sand. These corrosion studies concluded that neither inhibitor tested provided ideal mitigation of UDC, possibly a result of transport limitations through the sand bed and pre-corroded regions, but these conclusions were made without analyzing the interaction between neighboring electrodes. Tan, et al.,<sup>10</sup> used a partially sand-covered multi-electrode array, but focused on showing the interaction between the neighboring electrodes on a partially sand-covered multi-electrode array. Their experiments included measuring the galvanic current distribution without sand, under a partial sand deposit, and under a partial sand deposit with the addition of an imidazoline-type corrosion inhibitor. They confirmed that the addition of sand limits transport of corrosive species to the metal substrate under the deposit, but this limitation would not initiate localized corrosion. UDC resulted from inhibitor addition to the system. The addition of an imidazoline-type inhibitor at various concentrations from 10 ppm to 50 ppm was found to enhance localized

UDC as the potential difference between anodic and cathodic sites was measured to be approximately 250 mV, with major anodic areas found under the sand bed. In most of their experiments with industrial inhibitors relevant to oilfield applications, this type of galvanic corrosion could continue for more than 30 d. From these examples, the overall scenario for localized UDC to occur can be defined as a partial coverage by a wet inorganic deposit on the pipe wall with the presence of an inhibitor in the bulk fluid flow, which dramatically increases the probability to initiate and maintain a galvanic corrosion. However, pertinent research information toward understanding mitigation mechanisms was missing in these studies because the inhibitors did not have defined chemical components.

In research focused on the mechanisms of UDC, Huang<sup>3</sup> observed that pitting corrosion was initiated as a result of the inability of the corrosion inhibitor to protect the steel surface in the crevices immediately underneath each individual sand particle. In experiments using an imidazoline inhibitor package with all of the chemical components known, Huang concluded that the driving force for localized UDC was a result of galvanic effects between the larger cathodic area of the inhibited surface and the smaller anodic area underneath the sand particle that was not protected by the inhibitor. She also found that addition of thiosulfate enabled mitigation of this type of localized corrosion because of its lack of interaction with the silica sand. Through her research, Huang had developed a repeatable procedure to initiate localized UDC that could be used to test the effect of individual chemical components of an inhibitor on initiation of localized corrosion.

Phosphate esters (PE) are part of a class of anionic surface active components that are often added as components in corrosion inhibitors for well stimulations and oil and gas production, as they are effective at moderate temperatures or in the presence of trace amounts of oxygen.<sup>11</sup> Experiments by O'Lenick and Parkinson<sup>12</sup> found that ethoxylated surface active components had faster wetting times with 2 mol to 3 mol of ethylene oxide (EO) structural units added between each set of decyl alcohol hydrophobes and the phosphate head group. Wetting times decreased with an increase in the number of mol of EO present as intramolecular sub-units. They also found that as the number of carbon atoms was increased in the hydrophobic tail without EO, the wetting time increased.

Smith has described the role of intramolecular EO units as follows: "Some corrosion inhibitors are ethoxylated in order to increase the dispersibility of the chemical in water. The ethoxylation does not play a role in the actual inhibitor performance of the chemical other than allowing it to disperse into the aqueous phase so that it reaches the metal/water interface. Without ethoxylation, the oil soluble inhibitors would stay in the hydrocarbon liquid (or would

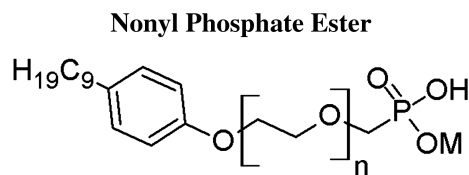


**FIGURE 1.** Chemical structure of nonyl phosphate mono-ester with location for  $n$  mol of ethylene oxide.

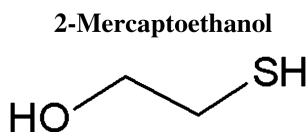


**FIGURE 2.** Chemical structure of 2-mercaptoethanol (ME).

float on the water/gas interface), where they will not inhibit the corrosion of the metal.”<sup>13</sup>

The chemical structure (Figure 1) for the mono-ester has the “M” shown on the phosphate head group present as hydrogen. For the di-ester, the “M” is the same hydrophobic tail ( $H_{19}C_9$ ) as is present in the mono-ester. The ethylene oxide (EO) is shown in brackets with the indicator “ $n$ ” for the number of EO mol in each branch. The number of EO mol defined in the text is related to the mono-ester; the di-ester would have the same number of EO mol in each branch of the ester. The nonylphenol PE tested had 9 mol to 10 mol of EO in each branch.

### Nonyl Phosphate Ester

2-mercaptoethanol ( $HOCH_2CH_2SH$ , abbreviated ME) is a hybrid of ethylene glycol that is added to inhibitor packages to enhance the adsorption and mitigation properties of longer chain, surfactant-like, inhibitors (Figure 2). UDC experiments have also found that ME can cause a reduction in both anodic and cathodic reactions under a 10 mm sand deposit.<sup>14</sup> Thiols are highly reactive molecules for a broad scope of chemical processes. The presence of ME is expected to dramatically decrease the likelihood of localized corrosion with respect to UDC, but the relationship between ME and specific PEs for corrosion mitigation in UDC is unknown.

### 2-Mercaptoethanol

Although studies have been conducted to understand how deposits form in order to mitigate deposit formation<sup>1-2</sup> and to experiment with inhibitor packages to understand the risk and mechanisms involved with inhibition of UDC,<sup>3,7-10</sup> no formal attempt has been made to observe the effects of specific chemical components in an inhibitor package on UDC. The objective of this study was to test individual chemical components used in industrial inhibitor packages against localized UDC. In this initial series of

experiments, the effect of varied ratios of mono- to dinonylphenol PEs were tested on the mitigation of UDC in sweet conditions. Three mono- to di-PE ratios were tested at 200 ppm with and without ME and at 100 ppm without ME.

## EXPERIMENTAL PROCEDURES

### Experimental Conditions

Experimentation for each inhibitor consisted of 28 d in a 2 L glass cell using API<sup>(1)</sup> 5L X65 pipeline steel partially covered with 250  $\mu$ m diameter sand particles. Experimental conditions required purging the specified brine (Table 1) with  $CO_2$  at 1 bar (100 kPa) total pressure while maintaining the solution temperature at 70°C. Prior to mounting in the UDC sample holder, each sample was polished to a 600-grit uniform surface finish, rinsed with isopropyl alcohol, and immersed in alcohol in a sonication bath to remove any loose material before being dried and weighed for testing. The UDC sample holder (Figure 3) had electrochemical connections for the sample that had sand on the surface, but the second sample did not have sand or electrochemical connections and was the control, or “blank,” sample. The electrochemical sample was mounted in the UDC sample holder specifically designed for this type of testing<sup>3</sup> and did not require any additional surface coating. The UDC sample holder uses an O-ring seal around the circumference of the electrochemical sample to isolate the spring-loaded electronic connection on the back of the sample to ensure it remains dry, while allowing the entire 7.9  $cm^2$  surface area to be exposed to the test solution. The “blank” or “weight loss” sample was coated on the sides and back with Teflon<sup>†</sup> paint so only the top circular 7.9  $cm^2$  surface area could corrode. After purging the solution for 3 h, the two 3.175 cm (1.25 in) diameter samples of X65 pipeline steel were mounted in this uniquely designed UDC sample holder<sup>3</sup> and then immersed in solution to begin the experiment.

For each experiment, the X65 samples experienced 2 h of pre-corrosion at open circuit potential (OCP). After the samples were immersed in solution, each experiment started with a pre-corrosion step to verify repeatable starting conditions for each test. To ensure a reproducible starting point, during the first hour of pre-corrosion, the initial corrosion rate was required to be in the range of  $3.1 \pm 0.5$  mm/y or the experiment would be abandoned. The OCP during the pre-corrosion for each experiment started at  $-680 \pm 20$  mV vs. an external Ag/AgCl reference electrode at 25°C, but would increase to a more positive value after the inhibitor was added. After completion of the first hour of pre-corrosion, sand that was stored in  $CO_2$  purged brine (Table 1) was transferred by pipette to the surface of the electrochemically monitored sample

<sup>(1)</sup> American Petroleum Institute, Washington, DC.

<sup>†</sup> Trade name.

**TABLE 1**  
Solution Mixture of Salts to Create the Desired Brine

Brine Composition		Component Salts for 3.4 wt% Brine		
Ion	ppm	Total Fluid:		2 L
		Salt	g/mol	Amount (g)
Na <sup>+</sup>	13,000	NaHCO <sub>3</sub>	84.007	0.85
Ca <sup>2+</sup>	95	NaCl	58.44	65.9
Mg <sup>2+</sup>	150	KCl	74.5513	0.39
Br <sup>-</sup>	-	CaCl <sub>2</sub> (anhydrous)	110.98	0.54
CH <sub>3</sub> COO <sup>-</sup>	600	Na <sub>2</sub> SO <sub>4</sub>	142.04	0.45
Cl <sup>-</sup>	20,000	NaCH <sub>3</sub> COO	82.0338	1.72
HCO <sub>3</sub> <sup>-</sup>	300	MgCl <sub>2</sub> · 6H <sub>2</sub> O	203.271	2.59
SO <sub>4</sub> <sup>2-</sup>	150			
TDS	34,295			

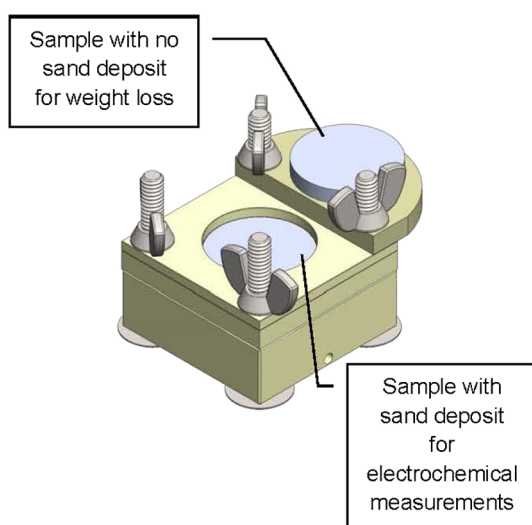


**FIGURE 3.** UDC sample holder showing location for electrochemical sample with sand coverage and weight loss sample without sand. Both samples have a 7.9 cm<sup>2</sup> (1.23 in<sup>2</sup>) wetted surface area.

for an approximate 25% surface coverage with a single layer of sand and then CO<sub>2</sub> purged model oil (LVT 200<sup>1</sup>) was added at 10% by volume to the glass cell. After another hour of monitoring pre-corrosion with the sand in place and the same range of corrosion rate maintained, the chosen inhibitor was added as ppm by total volume below the hydrocarbon phase in the 2 L glass cell. To minimize oxygen contamination, the CO<sub>2</sub> sparge rate was increased as additions to the glass cell were made through a 1 cm diameter opening in the lid.

Electrochemical data was collected on a daily basis and both samples were removed after 28 d for analysis. OCP, linear polarization resistance (Rp), and electrochemical impedance spectroscopy (EIS) measurements were collected manually on a daily basis. Automation of the electrochemical measurements was not used as added salts, inhibitors, and FeCO<sub>3</sub> precipitation have been found to interfere with the reference electrode connection to cause erroneous readings leading to possible damage of the working

electrode. The solution resistance (Rs) determined from EIS analysis was documented and used to correct the Rp calculation. Corrosion rate was calculated using a B value of 26 mV.

At the end of each experiment, a sample of the bulk solution below the hydrocarbon phase was taken for residual inhibitor analysis prior to removal of the samples for analysis. After removing them from solution, both samples were photographed, rinsed with nitrogen purged deionized water to remove salts and loose sand, rinsed with isopropyl alcohol to remove water, dried with a cool air blower, and stored in a desiccator until analyzed. Weight loss and image analysis procedures were conducted and recorded for each sample including scanning electron microscopy (SEM)/energy dispersive x-ray spectroscopy (EDS) of the corrosion product layer, corrosion product layer removal by Clarke solution cleaning,<sup>15</sup> and profilometer measurements of the metal surface to quantify any observable localized corrosion. After cleaning, each corrosion sample's surface was fully imaged with a profilometer to find the maximum pit depth. To determine the amount of residual inhibitor in the bulk solution after each experiment, surface tension measurements from a series dilution of each inhibitor (mN/m vs. ppm) were used as a guideline to back calculate the concentration of inhibitor from bulk solution collected at the end of the experiment before the samples were removed.

### Inhibitor Components

The chemical composition of each inhibitor in this study is listed in Table 2. Inhibitor packages numbered from 16 to 19 contained ME, while the inhibitor packages numbered from 26 to 29 did not contain ME.

## RESULTS AND DISCUSSION

The goals of these experiments were to observe if localized corrosion would initiate and propagate after the addition of a corrosion inhibitor to a system with a partial steel surface coverage by sand and if particular

**TABLE 2**  
*Chemical Composition of Tested Inhibitors*

Corrosion Inhibitor (CI) Number	Non-Phosphate Ester Active Components	Emulsion Breakers	ME	Solvent	Phosphate Ester (PE) 15%		No. of EO mol
					mono	di	
16	47.14%	4.75%	4.01%	44.1%		No PE	
17					90	10	
18	40.06%	4.04%	3.4%	37.49%	70	30	9-10
19					50	50	
26	47.14%	4.75%	0	48.11%		No PE	
27					90	10	
28	40.06%	4.04%	0	40.9%	70	30	9-10
29					50	50	

types of inhibitor components would influence mitigation properties. The first set of experiments was designed to observe the effect of the sulfur-containing species (ME) and the effect of the ratio of mono-PE to di-PE in the formulation using a 200 ppm by volume concentration of each inhibitor package in solution. Analysis of the samples from the first set of experiments confirmed that inhibitors without ME have a higher probability for pitting in UDC. Because the goal of these experiments was to observe the benefits and concerns of specific corrosion inhibitor components as related to UDC, the second set of experiments focused on the inhibitors that did not contain ME and used a lower concentration (100 ppm by volume) to increase the probability of localized corrosion related to UDC. Because of the 28-d test time, each experiment was not replicated in its entirety, but initial conditions for each experiment were highly scrutinized and the experiment was not allowed to continue if the environmental and electrochemical conditions did not fall within their respective specified range. Repeatability in analyzed results can be observed by the increase in localized corrosion as the ratio of mono-PE to di-PE decreased from 90:10 to 50:50 and the influence of the PE on the occurrence of localized corrosion.

### Set 1

*Sample Analysis* — All of the samples that were electrochemically monitored with the sand deposit in place for the first set of experiments are shown in Tables 3 through 5. At a 200 ppm concentration of inhibitor in solution, corrosion samples that were exposed to UDC conditions with ME in the inhibitor (Table 3) did not have any measureable localized corrosion. Some tarnishing of the surface was visible, but this would have occurred during the pre-corrosion step.

Corrosion samples that were exposed to UDC conditions without ME in the inhibitor experienced localized corrosion from 15  $\mu\text{m}$  to 120  $\mu\text{m}$  in depth over the 28-d exposure. There were only one or two locations of pitting observed on each of these samples

in Table 4, but the only difference in the inhibitor package was the lack of ME as compared to the samples in Table 3 that did not show any indication of localized corrosion. Although the general corrosion rates experienced by the samples were very low, the localized penetration rates show a correlation to the ratio of mono- to di-PE in the inhibitor. The localized corrosion rate was observed to increase with a decrease of mono-PE with a dramatic increase in rate observed between the 70:30 and the 50:50 mono- to di-PE ratios.

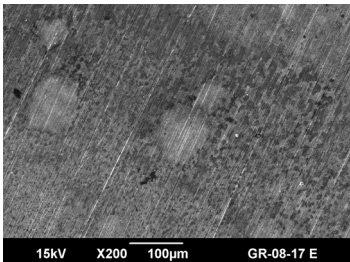
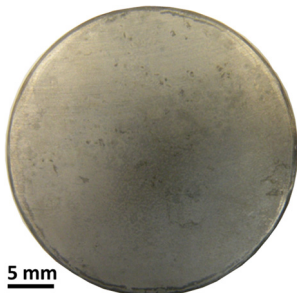
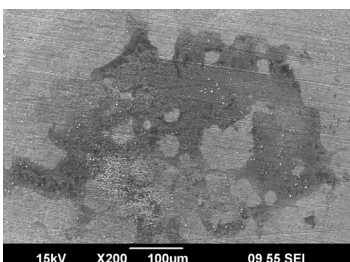
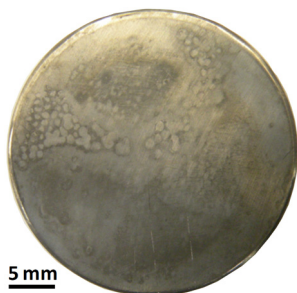
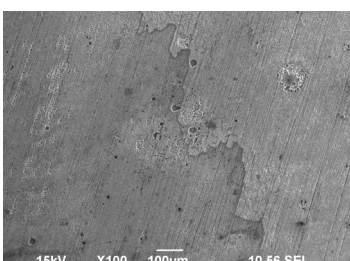
Corrosion samples that were exposed to UDC conditions without a PE in the inhibitor package also did not have any measureable localized corrosion. The samples in Table 5 were the electrochemically monitored samples with the sand deposit in place that were exposed to the base product of the inhibitor package, but without a PE. Neither of these samples showed indications of localized corrosion other than the initial tarnishing that occurred during pre-corrosion. The fact that the sample with no PE and no ME present did not show any characteristics of localized corrosion, similar to the samples shown in Table 4 with a PE and no ME, confirms the hypothesis that the molecularly larger surface active components of the inhibitor package are unable to protect the steel surface in the crevices immediately underneath each individual sand particle.

Although this seems to indicate that PEs should not be used in corrosion inhibitors when UDC is possible, many aspects must be taken into consideration during the formulation of corrosion inhibitors. Some PEs are added to mitigate corrosion in the presence of trace amounts of oxygen or to provide a cleaning effect to help remove debris in the system under which both UDC and bacterial attack can take place. Hence, the purpose of this work was to evaluate such PEs to determine and compare and contrast their efficiency at mitigating UDC as part of an overall package to attend to multiple corrosion threats.

*Electrochemical Measurements* — Review of the OCP data over the 28 d of each experiment does seem to

TABLE 3

Sample Surface Analysis After Removal from Experimental Conditions After 28 d Using ME-Containing Inhibitors with Varied Ratios of Mono- to Dinonylphenol PE at 200 ppm<sup>(A)</sup>

Inhibitor	Sample After Removal of Corrosion Product Layer	Representative Surface Features by SEM	Corrosion Information
CI(17) 90:10 with ME at 200 ppm			No localized material loss. Weight loss corrosion rate: 0.0049 mm/y (0.19 mpy).
CI(18) 70:30 with ME at 200 ppm			No localized material loss. Weight loss corrosion rate: 0.0027 mm/y (0.11 mpy).
CI(19) 50:50 with ME at 200 ppm			No localized material loss. Profilometer depth measurements were less than 10 μm depth. Weight loss corrosion rate: 0.0026 mm/y (0.10 mpy).

(A) 70°C, 3.4 wt% brine solution, 1 bar (100 kPa) total pressure, continuous purge with CO<sub>2</sub>, pH 6.

give an indication of whether or not pitting occurred during the experiment. Although the OCP for each experiment was only measured once per day, the fluctuations in these values during the last 20 d of each experiment seemed to indicate a higher probability of localized corrosion. Moloney, et al.,<sup>16</sup> found that potential transients in a continuously measured OCP can be directly attributed to pitting activity on the metal surface. Although the data in this current study only reviewed the OCP on a daily basis, when the OCP was not stable (more than ±10 mV fluctuation) during the 28 d experiments, the sample was more likely to have measurable localized corrosion.

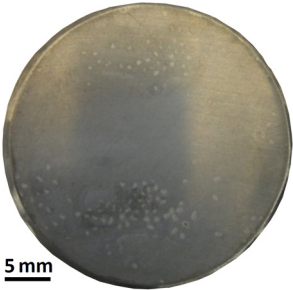
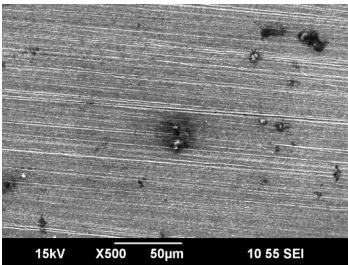
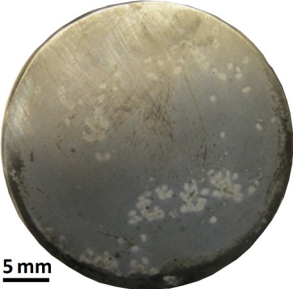
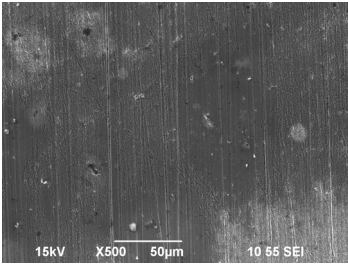
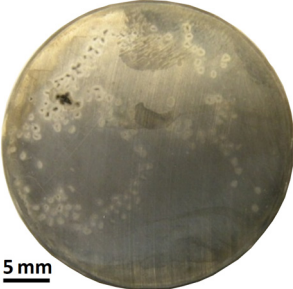
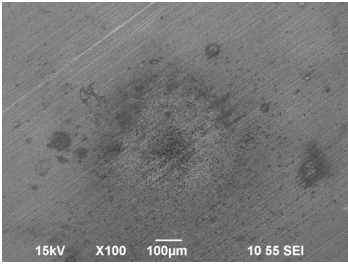
The comparison of electrochemical measurements in Figures 4 and 5 agree with this assumption. The general corrosion rate seems stable in both cases, but the OCP for CI(29) in Figure 4 experienced fluctuations up to 16.7 mV during the last 20 d of the experiment. The sample with CI(29) containing 50:50

mono- to dinonylphenol PE with no ME experienced localized corrosion measured at 120 μm in depth (Table 4). The sample with CI(19) containing 50:50 mono- to dinonylphenol PE with ME had a maximum change in potential of 5.7 mV over the last 20 d of the experiment with no true visual indication of localized corrosion (Table 3).

*Effect of Inhibitor Components* — At 200 ppm concentration, each inhibitor package did provide protection against general corrosion, but it was observed that the inhibitors without the ME additive show a higher probability for UDC localized corrosion. It was also observed that the CI(29) inhibitor package with a 50:50 ratio of mono- to dinonylphenol PE and no ME had the largest pit penetration rate of localized corrosion under these conditions. Notice that the change in local penetration rate for CI(29) is more than 1.5 times greater than a linear relationship to the increasing concentration of di-PEs, which indicates a preference

TABLE 4

Sample Surface Analysis After Removal from Experimental Conditions After 28 d Using Inhibitors Without ME at Varied Ratios of Mono- to Dinonylphenol PE at 200 ppm<sup>(A)</sup>

Inhibitor	Sample After Removal of Corrosion Product Layer	Representative Surface Features by SEM	Corrosion Information
CI(27) 90:10 no ME at 200 ppm			Localized material loss found at 15 μm depth. Penetration rate: 0.2 mm/y. Weight loss corrosion rate: 0.0032 mm/y (0.13 mpy).
CI(28) 70:30 no ME at 200 ppm			Localized material loss found at 45 μm depth. Penetration rate: 0.6 mm/y. Weight loss corrosion rate: 0.0066 mm/y (0.26 mpy).
CI(29) 50:50 no ME at 200 ppm			Localized material loss found at 120 μm depth. Penetration rate: 1.75 mm/y. Weight loss corrosion rate: 0.0052 mm/y (0.020 mpy).

<sup>(A)</sup> 70°C, 3.4 wt% brine solution, 1 bar (100 kPa) total pressure, continuous purge with CO<sub>2</sub>, pH 6.

for using higher mono- to di-PE ratios for inhibitors to be used in UDC mitigation.

The surface tension measurements conducted with the solution from the end of each experiment were to be used to measure the concentration of residual inhibitor and to observe any differences in concentration for explanation of inhibitor losses during each experiment. Although the measured amount of residual inhibitor in solution at the end of each experiment was less than 50% of the original concentration, there was little difference in the overall measured concentrations of residual inhibitor (43±3%) from all eight experiments. This negated the possibility that a change in inhibitor concentration would influence which X65 samples experienced localized corrosion.

Overall, it was understood that a 200 ppm inhibitor concentration was too high to observe the effect of changing parameters with ME present, but,

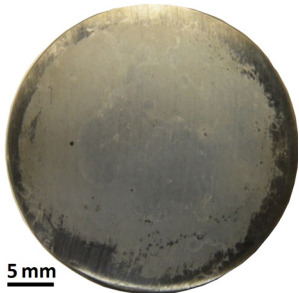
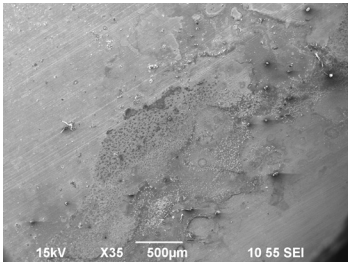
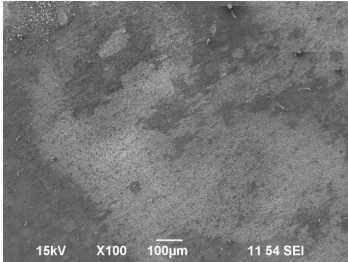
without ME, it was observed that the ratio of mono- to di-PEs did have an effect on mitigation of localized corrosion initiation. This led to a second set of experiments at a lower inhibitor concentration in order to confirm the results of Set 1 and to observe if the pitting rate would increase by challenging the inhibitors at a lower dosage.

### Set 2

**Sample Analysis** — All of the samples that were electrochemically monitored with the sand deposit in place for the second set of experiments are shown in Table 6. At a 100 ppm concentration of inhibitor in solution, the corrosion samples that were exposed to UDC conditions for the nonylphenol PE without ME had localized corrosion features ranging from 55 μm to 113 μm in depth (Table 6). With one half of the inhibitor concentration from Set 1, the general weight

TABLE 5

Sample Surface Analysis After Removal from Experimental Conditions After 28 d Using Base Product Inhibitors at 200 ppm<sup>(A)</sup>

Inhibitor	Sample After Removal of Corrosion Product Layer	Representative Surface Features by SEM	Corrosion Information
CI(16) No PE with ME at 200 ppm			No localized material loss. Profilometer depth measurements were less than 10 µm depth. Weight loss corrosion rate: 0.0030 mm/y (0.12 mpy).
CI(26) No PE no ME at 200 ppm			No localized material loss. Profilometer depth measurements were less than 10 µm depth. Weight loss corrosion rate: 0.0030 mm/y (0.12 mpy).

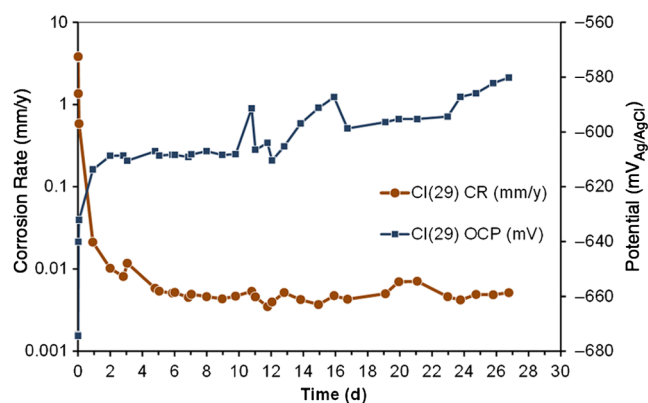
<sup>(A)</sup> 70°C, 3.4 wt% brine solution, 1 bar (100 kPa) total pressure, continuous purge with CO<sub>2</sub>, pH 6.

FIGURE 4. Open circuit potential (OCP) and corrosion rate (CR) for CI(29) (50:50 mono- to dinonylphenol PE with no ME) at 200 ppm.

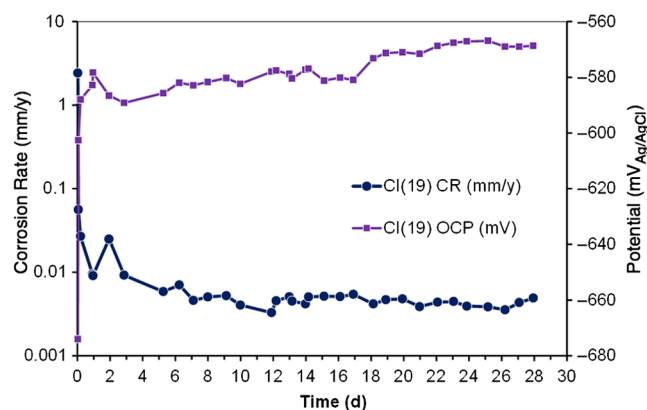


FIGURE 5. Open circuit potential (OCP) and corrosion rate (CR) for CI(19) (50:50 mono- to dinonylphenol PE with ME) at 200 ppm.

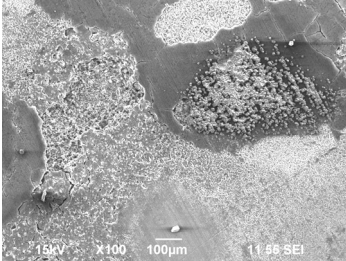
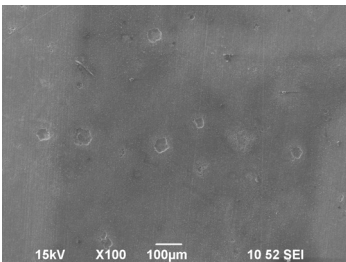
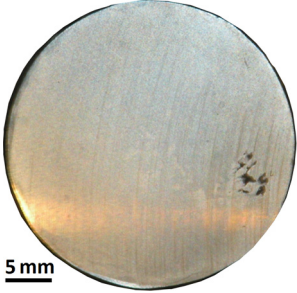
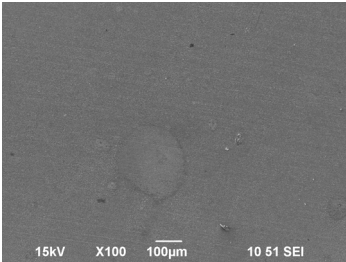
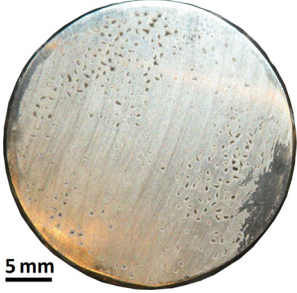
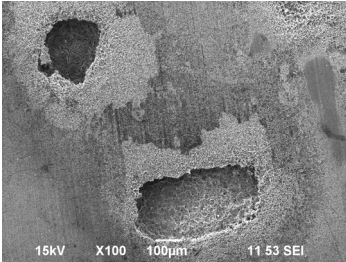
loss increased by a factor of 3 for CI(28) to a factor of 10 for CI(26). Although the general weight loss for each sample exposed to an inhibitor with a PE was still less than 0.025 mm/y (1 mpy), there was a significant increase in the amount of localized corrosion as the ratio of mono- to di-PE decreased from 70:30 to 50:50. This is the same phenomenon that was observed for the same inhibitors at a 200 ppm concentration in solution.

The samples taken from the experiment with CI (29) at 100 ppm are shown in Figures 6 and 7. These samples were removed from the experiment and carefully rinsed with deoxygenated isopropyl alcohol

before being photographed. The sand is shown on the electrochemical sample in the image at the bottom of Figure 6. The same electrochemical sample after its recovery from the sample holder with the sand removed is shown in Figure 7. The intact corrosion product layer shows the locations where pitting and localized corrosion occurred. Profilometer measurements in Figure 8 were conducted after the corrosion product was removed and show the maximum pit penetration to be 113 µm, which is equivalent to 1.5 mm/y penetration rate. The weight loss sample used for comparison without sand or electrochemical measurements (top of Figure 6) did not have any localized corrosion.

TABLE 6

Sample Surface Analysis After Removal from Experimental Conditions After 28 d Using Inhibitors Without ME at Varied Ratios of Mono- to Dinonylphenol PE or no PE at 100 ppm<sup>(A)</sup>

Inhibitor	Sample After Removal of Corrosion Product Layer	Representative Surface Features by SEM	Corrosion Information
CI(26) No PE no ME at 100 ppm			Localized material loss found at 55 µm depth. Penetration rate: 0.72 mm/y. Weight loss corrosion rate: 0.030 mm/y (1.18 mpy).
CI(27) 90:10 no ME at 100 ppm			Localized material loss found at 65 µm depth. Penetration rate: 0.85 mm/y. Weight loss corrosion rate: 0.014 mm/y (0.55 mpy).
CI(28) 70:30 no ME at 100 ppm			Localized material loss found at 99 µm depth. Penetration rate: 1.3 mm/y. Weight loss corrosion rate: 0.020 mm/y (0.79 mpy).
CI(29) 50:50 no ME at 100 ppm			Localized material loss found at 113 µm depth. Penetration rate: 1.5 mm/y. Weight loss corrosion rate: 0.017 mm/y (0.67 mpy).

<sup>(A)</sup> 70°C, 3.4 wt% brine solution, 1 bar (100 kPa) total pressure, continuous purge with CO<sub>2</sub>, pH 6.

As compared to similar samples tested with nonylphenol PE at different mono- to di- ratios, the weight loss corrosion rate was higher for inhibitor CI(26) without PE at 100 ppm (Table 6). This was also thought to be the reason for a minimal amount of localized corrosion on this sample, which was about the same as the 90:10 mono- to dinonylphenol PE when taking into account the increase in general corrosion rate.

*Electrochemical Measurements* — The second set of experiments was conducted identically to the first set with the OCP, Rp, and EIS data collected on a daily basis over the 28-d experimental duration. The Rs was determined from EIS analysis and used to correct the corrosion rate calculations. After 2 h of pre-corrosion with initial corrosion rates at 3.1±0.5 mm/y, a partial coverage of sand was added to the electrochemical sample and then the inhibitor. Review of the OCP data

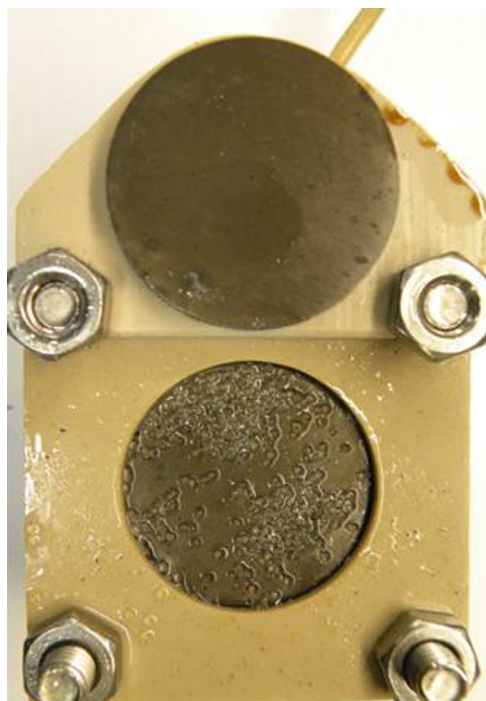


**FIGURE 6.** Samples in sample holder “as-removed” from the experiment for inhibitor CI(29) at 100 ppm.



**FIGURE 7.** Electrochemical sample with corrosion product layer after removal of the sand particles for the experiment with inhibitor CI(29) at 100 ppm.

over the 28 d of the experiment with inhibitor CI(28) (Figure 9) and inhibitor CI(29) (Figure 10) did not give a clear indication whether or not pitting occurred during the experiment, although both experienced fluctuations in the OCP greater than 10 mV. The electrochemical sample with CI(28) had a maximum potential fluctuation of 15.3 mV during the last 20 d of the experiment, while the sample with CI(29) had a maximum potential fluctuation of 11.7 mV. Both of these inhibitors showed similar trends in corrosion rate,

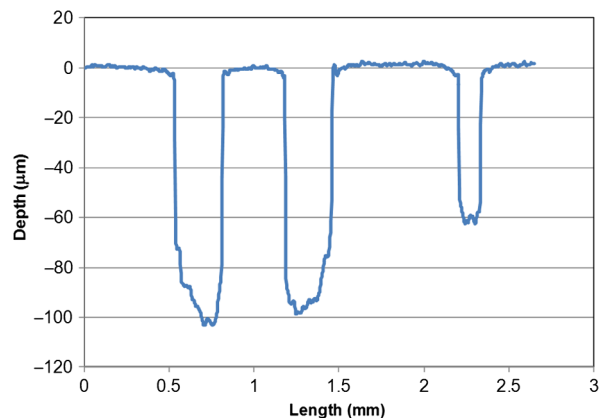


**FIGURE 8.** Profilometer measurements of localized corrosion at depths of 101  $\mu\text{m}$ , 98.4  $\mu\text{m}$ , and 61  $\mu\text{m}$ , respectively, found on electrochemical sample after experiment with inhibitor CI(29) at 100 ppm.

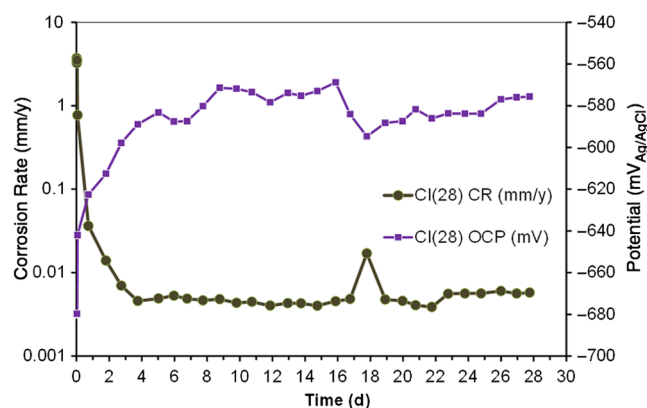


**FIGURE 9.** Open circuit potential (OCP) and corrosion rate (CR) for CI(28) (70:30 mono- to dinonylphenol PE with no ME) at 100 ppm.

solution resistance, and OCP measurements, although the results were quite different.

**Effect of Inhibitor Components** — The general corrosion rate for all four experiments at 100 ppm inhibitor had values that were a factor of 3 to 10 times higher than at 200 ppm. Inhibitors CI(26) (base product), CI(27) (90:10 mono- to di-PE), and CI(28) (70:30 mono- to di-PE) experienced deeper penetration rates for localized corrosion at 100 ppm than at 200 ppm concentration, but all of these had limited onset of localized events (one to three pits). Inhibitor CI(29) (50:50 mono- to di-PE) failed to protect the surface of the sample under the individual sand grains. There was so much difference between the CI(29) at 100 ppm and the other three inhibitors tested in Set 2 that it proves a major decrease in mitigation of UDC occurs between the 70:30 mono- to di-PE and the 50:50 mono- to di-PE.

Residual inhibitor concentration at the end of the Set 2 experiments was measured at  $34 \pm 5\%$  of the original concentration in the bulk solution. But this decrease of excess inhibitor available in the bulk

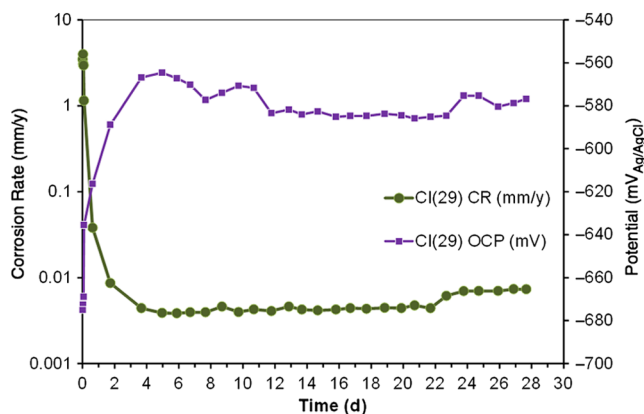


**FIGURE 10.** Open circuit potential (OCP) and corrosion rate (CR) for CI(29) (50:50 mono- to dinonylphenol PE with no ME) at 100 ppm.

solution, again, did not have any correlation to the observations of localized corrosion, which negates the possibility that a change in bulk inhibitor concentration during the experiments would influence which X65 samples experienced localized corrosion.

## CONCLUSIONS

- ❖ The presence of 2-mercaptoethanol (ME) almost always assisted the nonylphenol PE inhibitors to have better performance. When such a sulfur-containing compound was present in the inhibitor used at 200 ppm by volume, no localized corrosion was observed.
- ❖ Localized corrosion (pit penetration rate) increased for nonylphenol PEs without ME as the amount of diphosphate esters became equivalent to the concentration of monophosphate esters: CI(27) (90:10 mono- to di-PE) 15  $\mu\text{m}$  pitting, CI(28) (70:30 mono- to di-PE) 45  $\mu\text{m}$  pitting, and CI(29) (50:50 mono- to di-PE) 120  $\mu\text{m}$  pitting, which indicates a preference for using higher mono- to di-PE ratios in inhibitor formulations to be used in UDC mitigation.
- ❖ The 50:50 mono- to dinonylphenol PE inhibitor, CI (29), at 100 ppm concentration failed to protect the surface of the sample under the individual sand grains.
- ❖ From this research, it is seen that the mono- to diphosphate ester ratio is important to consider when developing corrosion inhibitors containing phosphate esters, which may be added to attend to multiple

corrosion threats, to mitigate UDC. A higher mono- to diphosphate ester ratio increases the efficacy in UDC inhibition and in turn enhances the versatility of the product, enabling it to be used under a wider range of operating environments.

## ACKNOWLEDGMENTS

This research was conducted at the Institute for Corrosion and Multiphase Technology, Ohio University, with financial support and cooperation by NALCO Champion. The authors would like to thank NALCO Champion for permission to present these results.

## REFERENCES

1. X. Landry, A. Runstedtler, S. Papvinasam, T. Place, *Corrosion* 68, 10 (2012): p. 904-913.
2. A. Runstedtler, P. Boisvert, T. Place, *Corrosion* 71, 6 (2015): p. 726-734.
3. J. Huang, "Mechanistic Study of Under Deposit Corrosion of Mild Steel in Aqueous Carbon Dioxide Solution" (Ph.D. diss., Ohio University, 2013).
4. J. Vera, D. Daniels, M. Achour, "Under Deposit Corrosion (UDC) in the Oil and Gas Industry: A Review of Mechanisms, Testing and Mitigation," CORROSION 2012, paper no. 1379 (Houston, TX: NACE International, 2012).
5. M.M. Salama, "Influence of Sand Production on Design and Operations of Piping Systems," CORROSION 2000, paper no. 80 (Houston, TX: NACE, 2000).
6. J.S. Smart, *Pipeline & Gas J.* 231, 10 (2004): p. 28-30.
7. J. Marsh, J.W. Palmer, R.C. Newman, "Evaluation of Inhibitor Performance for Protection Against Localized Corrosion," CORROSION 2002, paper no. 288 (Houston, TX: NACE, 2002).
8. A. Pedersen, K. Bilkova, E. Gulbrandsen, J. Kvarekvål, "CO<sub>2</sub> Corrosion Inhibitor Performance in the Presence of Solids: Test Method Development," CORROSION 2008, paper no. 632 (Houston, TX: NACE, 2008).
9. G. Hinds, A. Turnbull, *Corrosion* 66, 4 (2010): p. 046001-1 to 046001-10.
10. Y. Tan, Y. Fwu, K. Bhardwaj, *Corros. Sci.* 53 (2011): p. 1254-1261.
11. B. Alink, B. Outlaw, V. Jovancevic, S. Ramachandran, S. Campbell, "Mechanism of CO<sub>2</sub> Corrosion Inhibition by Phosphate Esters," CORROSION 1999, paper no. 037 (Houston, TX: NACE, 1999).
12. A.J. O'Lenick, J.K. Parkinson, *Textile Chemist & Colorist* 27, 11 (1995): p. 17-20.
13. S. Smith, correspondence to author, August 2014.
14. R. Barker, B. Pickles, A. Neville, "General Corrosion of X65 Steel Under Silica Sand Deposits in CO<sub>2</sub>-Saturated Environments in the Presence of Corrosion Inhibitor Components," CORROSION 2014, paper no. 4215 (Houston, TX: NACE, 2014).
15. ASTM Standard G1, "Standard Practice for Preparing, Cleaning, and Evaluating Corrosion Test Specimens" (West Conshohocken, PA: ASTM International, 2003).
16. J.J. Moloney, W.Y. Mok, C.M. Menendez, *Corrosion* 66, 6 (2010): p. 065003-1 to 065003-18.